Structural, elastic, electronic, and magnetic properties of quaternary alloys $BBi_{0.75}Mn_{0.125}N_{0.125}$: A first-principles study

S. Tab[a], A. Boudali[a], M. Berber[b,c,*], M. Driss Khodja[a], O. Lhaj El Hachemi[d], H. Moujri[e]

[a]*Laboratory of Physico-chemical Studies, University of Saida, Algeria.*

[b]*Centre Universitaire Nour Bachir El Bayadh, 32000 El Bayadh, Algérie.*

e-mail: berbermohamed@yahoo.fr

http://orcid.org/0000-0003-1285-3070

[c]*Laboratoire d'Instrumentation et Matériaux Avancés, Centre Universitaire Nour Bachir El-Bayadh, BP 900 route Aflou, 32000, Algérie.*

[d]*LPMMAT, Faculty of Sciences Ain Chock, Hassan II University of Casablanca, Morocco.*

[e]*Renewable Energy Laboratory and dynamic systems, Faculté des Sciences Ain-Chock, Université Hassan II de Casablanca, Morocco.*

Received 31 May 2020; accepted 7 July 2020

In this study, we have employed the first-principle methods based on density functional theory to investigate the structural, elastic, electronic, and magnetic properties of $BBi_{0.75}Mn_{0.125}N_{0.125}$. The exchange and correlation potential are described by the generalized gradient approximation of Perdew, Burke, and Ernzerhof (GGA-PBEsol) + SOC coupled with TB-mBJ approaches. The studied structure shows that the compound $BBi_{0.75}Mn_{0.125}N_{0.125}$ is stable in the ferromagnetic phase, the elastic property indicates that the structure is brittle and mechanically stable. The half-metallic description is predicted with the energy spin bandgap in the spin-up channel. The structure attributed to half-metallic ferromagnetism could be suitable for spintronics devices. To our knowledge, this is the first time that a study has been done on this alloy, and we would like it to serve as a reference for the next studies.

Keywords: First-principles computation; GGA-PBEsol approximation; SOC; TB-mBJ; magnetic properties.

PACS: 71.15.Mb; 71.20.-b; 74.25.Ha

DOI: https://doi.org/10.31349/RevMexFis.66.627

1. Introduction

Since the discovery of the spin at the beginning of the last century [1-3], which was an inflection point and a profound change for semiconductor applications. After some years, a new discipline was created in physics to study electron spin: it is spintronics. The importance of applications of spintronics or magnetoelectronics is store information and the giant magnetoresistance (GMR) for drive head technology [4]. To manufacture the components intended for spintronics, the researchers doped the semiconductor by transition elements, when will later call them DMSs (the dilute magnetic semiconductors). The first DMSs $In_{1-x}Mn_xAs$ was produced by a molecule beam epitaxy (MBE) [5]. Nevertheless, work has not stopped and is still rising; in the last decade many researchers are working on diluted magnetic III-V and II-VI semiconductors for spintronics applications [6-12]. The magnetic properties of Heusler are calculated by several researchers [13-18]. Researchers and scientists pursue another work line to identify other spintronic components and between these axes the ternaries II-VI and III-V doped with a metallic element [19-20]. The essential intention of this article is to predict the half-metallic property in III-V-N alloy, by doping of transition metal atom manganese, we have chosen the following quaternary $BBi_{0.75}Mn_{0.125}N_{0.125}$ alloy.

2. Calculation details

Developed on full potential linearized augmented plane wave (FP-LAPW) method in accordance with the framework of DFT (density functional theory) [21] electronic structure, half-metallic behavior, and magnetic properties were investigated using WIEN2k code [22-24]. Generalized gradient approximation within Perdew-Burke-Ernzerhof (PBEsol) [25] approximation was employed for exchange-correlation, jointed with the modified Becke-Johnson (mBJ) potential [26] and also spin-orbit coupling (SOC) [27-29] was applied. Boron-Bismuth (BBi) crystallizes in the zincblende structure (no. 216) [27-29]. Its conventional structure has two types of atoms, B and Bi, located at (0,0,0) and (0.25,0.25,0.25) positions, respectively. We create a supercell of 16 atoms, 8 atoms for Boron (B) and 8 for Bismuth (Bi), we substituted one atom of Manganese (Mn), and one atom of Nitrogen (N) at Bismuth (Bi) sites to create $BBi_{0.75}Mn_{0.125}N_{0.125}$ zincblende structure. In this article, we have designed the following calculation parameters: the muffin-tin radii (MT) for B, Bi, Mn, and N to be 1.64, 2.39, 2.29, and 2.13 atomic units (a.u.), respectively. The $K_{\max} = 9$ (RMT)$^{-1}$ ($K_{\max}$ is the plane wave cut-off, and RMT is the smallest of all atomic sphere radii). The Fourier expanded charge density was truncated at $G_{\max} = 12$ (Ryd)$^{1/2}$, the l-expansion of the non-

TABLE I. Calculated lattice constant (a), bulk modulus (B), pressure derivative B', minimum equilibrium energy E_0, and equilibrium volume V_0 $BBi_{0.75}Mn_{0.125}N_{0.125}$.

a (Å)	B (GPa)	B'	Energy E_0 (Ry)	Volume V_0 (a.u^3)	Character
10.5096	91.3200	4.6243	-261728.202334	1961.0587	Ferromagnetic
10.4686	91.4098	4.6388	-261728.130051	1935.5166	Non-magnetic

spherical potential and charge density was carried out up to $l_{\max} = 10$. The cut-off energy is set to -6 Ryd to separate the core from valence states. The self-consistent calculations are judged to be converged when the total energy of the system is stable within 10^{-4} Ryd.

3. Results and discussions

3.1. Phase stability, Structural and elastic properties

To confirm the phase stability of the structure, we carried out the volume optimization and plotted the energy as a function of the volume for both magnetic and non-magnetic cases. Figure 1 exhibit the energy as a function of the volume. For the ferromagnetic curve localized under to non-magnetic curv, it is concluded that the compound contains the minimum energy in the ferromagnetic phase compared to the non-magnetic phase, which indicates that the $BBi_{0.75}Mn_{0.125}N_{0.125}$ alloy is stable in ferromagnetic phase. The ground-state properties such as the equilibrium lattice constant a, the bulk modulus B_0, the bulk modulus pressure derivative B', minimum equilibrium energy E_0, and equilibrium volume V_0, are presented in Table I.

The derivative of the energy as a function of the lattice strain is essential for knowing the elastic constants [30]. This strain is picked so that the volume of the unit cell is saved, for the situation of the cubic framework. Along these lines, for the figuring of flexible constants: C_{11}, C_{12}, and C_{44}, we have utilized the Mehl strategy [31], Following this technique, we determined the shear modulus $C_{11} - C_{12}$ from the volume-preserving orthorhombic strain tensor:

$$\begin{bmatrix} 1+\delta & 0 & 0 \\ 0 & 1-\delta & 0 \\ 0 & 0 & 1/(1-\delta^2) \end{bmatrix}. \quad (1)$$

Utilization of this strain changes the total energy from its unstrained value to:

$$E(\delta) = E(-\delta) = E(0) + (C_{11} - C_{12})V_0\delta^2 + O(\delta^4), \quad (2)$$

Where V_0 is the volume of the unstrained equilibrium unit cell, and $E(0)$ is its total energy. For the elastic constant C_{44}, we used a volume-conserving monoclinic tensor.

$$\begin{bmatrix} 1 & \delta/2 & 0 \\ \delta/2 & 1 & 0 \\ 0 & 0 & 4/(4-\delta^2) \end{bmatrix}. \quad (3)$$

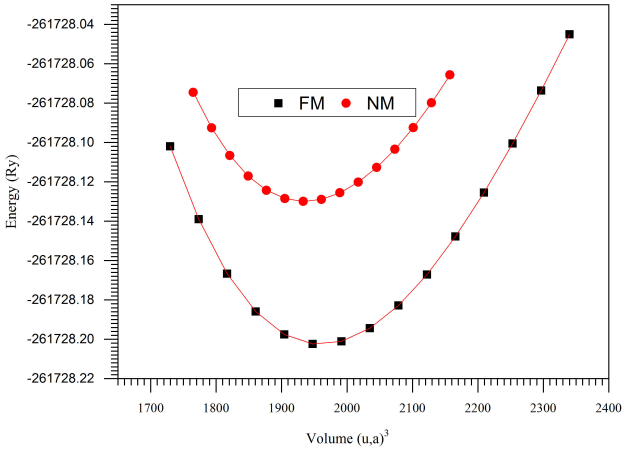

FIGURE 1. Volume optimization curve of $BBi_{0.75}Mn_{0.125}N_{0.125}$ structure

Which changes the total energy to:

$$E(\delta) = E(-\delta) = E(0) + \frac{1}{2}C_{44}V_0\delta^2 + O(\delta^4). \quad (4)$$

For isotropic cubic crystal, the bulk modulus B is given by:

$$B = \frac{1}{3}(C_{11} + 2C_{12}). \quad (5)$$

The Young's modulus E, shear modulus G, and Lame's coefficients (μ and λ) can be derived from the elastic constants, using the following standard relations:

$$E = \frac{9BG}{(3B+G)}, \quad (6)$$

$$G = \frac{(C_{11} - C_{12} + C_{44})}{5} \quad (7)$$

$$\mu = \frac{E}{(2(1+\sigma))}. \quad (8)$$

$$\lambda = \frac{\sigma E}{((1+\sigma)(1-2\sigma))}. \quad (9)$$

Similarly, the Poisson coefficient (σ) provides information on the ductility or fragility of the materials and is expressed as follows:

$$\sigma = \frac{1}{2} - \frac{E}{6B}. \quad (10)$$

The anisotropy factor is given by the following equation:

$$A = \frac{2C_{44}}{C_{11} - C_{12}}. \quad (11)$$

TABLE II. The calculated elastic constants of the $BBi_{0.75}Mn_{0.125}N_{0.125}$.

C_{11}	143.008 (GPa)
C_{12}	65.375 (GPa)
$4C_{44}$	102.444 (GPa)
B	91.252 (GPa)
G_V	76.993 (GPa)
G_R	61.874 (GPa)
G_H	69.433 (GPa)
E	166.158 (GPa)
B/G	1.314
A	2.639
σ	0.196
μ	69.433 (GPa)
λ	44.963 (GPa)
v_t	2936.280 (m/s)
v_l	4777.730 (m/s)
v_m	3240.400 (m/s)
θ_D	367.017 (K)

Stability criteria for cubic crystals require [32]:

$$C_{11} - C_{12} > 0, \quad C_{11} > 0, \quad C_{44} > 0,$$
$$C_{11} + 2C_{12} > 0, \quad C_{12} < B < C_{11}. \tag{12}$$

These conditions in our study are satisfying, and the structure is therefore mechanically stable. The calculated values of the elastic constants (C_{11}, C_{12} and, C_{44}), shear modulus G, Young's modulus E, the anisotropy A, Poisson's ratio σ, and Lame's coefficients (μ and λ) are given in Table II.

Acquiring calculated Young's modulus E, bulk modulus B, and shear modulus G, one can estimate the Debye temperature, which is an important fundamental parameter closely related to many physical properties such as elastic constants, specific heat, and melting temperature. One of the main technique to predict the Debye temperature (θ_D) is from elastic constants data, since θ_D may be estimated from the average sound velocity, v_m by the following expression [33]:

$$\theta_D = \frac{h}{k_B}\left[\frac{3n}{4\pi V_a}\right]^{1/3} v_m. \tag{13}$$

Where h is Plank's constant, k_B Boltzmann's constant, and V_a is the atomic volume. The standard sound velocity in the polycrystalline material is given by [34]:

$$v_m = \left[\frac{1}{3}\left(\frac{2}{v_l^3} + \frac{1}{v_l^3}\right)\right]^{1/3} \tag{14}$$

where v_l and v_t are the longitudinal and transverse sound velocity in an isotropic material which can be attained using

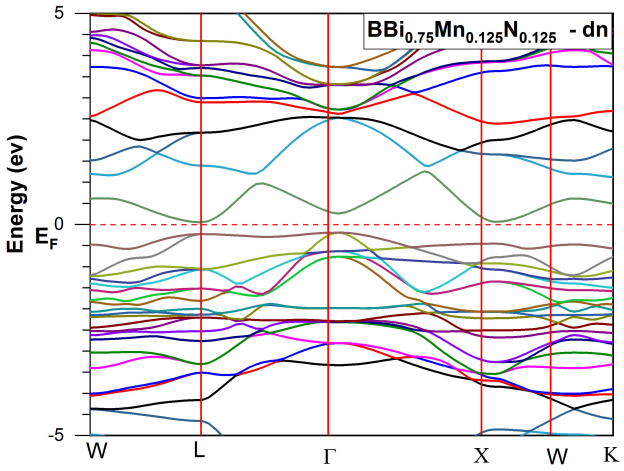

FIGURE 2. Spin-polarized band structure obtained with TB-mBJ for $BBi_{0.75}Mn_{0.125}N_{0.125}$: for majority spin (up). The Fermi level is set to zero (horizontal dotted red line).

the shear modulus G and the bulk modulus B from Navier's formula [35]:

$$v_l = \left(\frac{3B + 4G}{3\rho}\right)^{1/2} \quad \text{and} \quad v_t = \left(\frac{G}{\rho}\right)^{1/2}. \tag{15}$$

The calculated sound velocity and Debye temperature are given in Table II. However, to our knowledge, there are no data available related to these properties in the literature for these compounds. Pugh [36] propose the ratio B/G, a relationship related to brittle or ductile behavior of materials a high B/G ratio is associated with ductility, whereas a low value corresponds to the brittleness. The critical value separating ductile and brittle material is 1.75; the ratio B/G is 1.314 for $BBi_{0.75}Mn_{0.125}N_{0.125}$, so the structure is brittle.

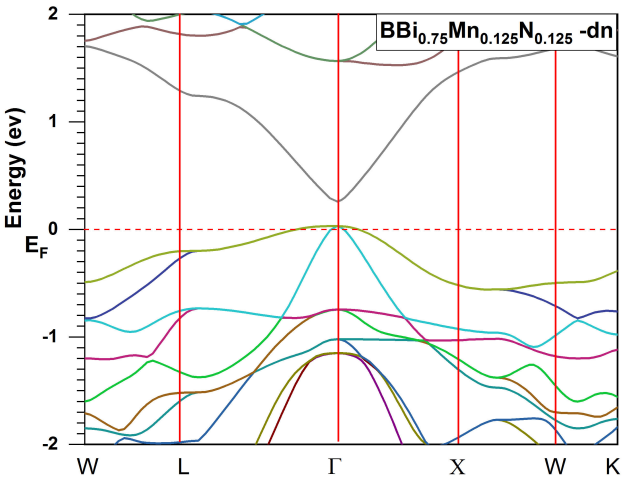

FIGURE 3. Spin-polarized band structure obtained with TB-mBJ for $BBi_{0.75}Mn_{0.125}N_{0.125}$: for minority spin (dn). The Fermi level is set to zero (horizontal dotted red line).

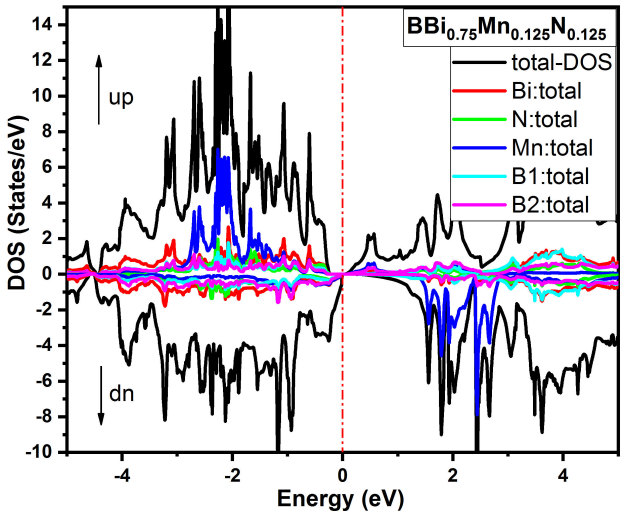

FIGURE 4. Spin-polarized total and partial densities of states of $BBi_{0.75}Mn_{0.125}N_{0.125}$. The Fermi level is set to zero (vertical dotted red line).

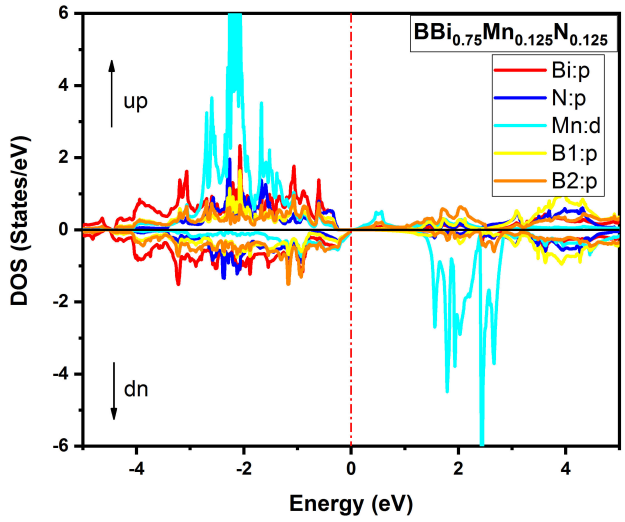

FIGURE 5. Spin-polarized partial densities of states of $BBi_{0.75}Mn_{0.125}N_{0.125}$. The Fermi level is set to zero (vertical dotted red line).

3.2. Electronic properties and half-metallic behavior

In this part, we present the electronic band structure, total and partial densities of states for $BBi_{0.75}Mn_{0.125}N_{0.125}$ using the GGA-PBEsol and TB-mBJ approaches. Figure 2 exhibits the spin-polarized band structure obtained with TB-mBJ for $BBi_{0.75}Mn_{0.125}N_{0.125}$ for majority spin (spin-up). It is observed that the half-metallic gap is seen in the spin-up channel, the indirect bandgap is about 0.25 eV between the Γ and L high symmetry points. Figure 3 shows the band structure for $BBi_{0.75}Mn_{0.125}N_{0.125}$ for minority spin (spin down), it is clear that the maximum of the valence band is above the Fermi level, therefore the structure has metallic behavior. The total (T) and partial (P) electron densities of states of $BBi_{0.75}Mn_{0.125}N_{0.125}$ are shown in Fig. 4 and Fig. 5, respectively. Figure 3 shows that $BBi_{0.75}Mn_{0.125}N_{0.125}$ compound present half-metallic ferromagnetic comportment as the density of states (DOS) passes Fermi level in the spin-down version, and it is also clear from the figure that the peaks around -1.8 eV are mainly contributed by the total density states of Mn. The partial density of states (PDOS) of $BBi_{0.75}Mn_{0.125}N_{0.125}$ is presented in Fig. 4, and it is more apparent that 3d states of Mn largely implicated in the peaks around -1.81 and 2.80 eV. The energy gap is acquired resulting from the hybridization of the 3d-state of Mn, p-state of Bi, and p state of N, as shown in Fig. 4. The half-metallic ferromagnetic behavior of $BBi_{0.75}Mn_{0.125}N_{0.125}$ imply applications of the structure in the spintronic devices.

4. Conclusion

In this paper, the GGA-PBEsol coupled with TB-mBJ study to investigate the elastic, electronic and magnetic properties within the framework of density functional theory based on FP-LAPW method. The results show that $BBi_{0.75}Mn_{0.125}N_{0.125}$ structure is stable in the ferromagnetic phase and mechanically. The compound has half-metallic ferromagnetic and can be used in spintronics applications. From our knowledge, there are no previous theoretical or experimental studies on the $BBi_{0.75}Mn_{0.125}N_{0.125}$ material, thus we hope that our results serve as a reference for future theoretical and experimental research.

1. G. E. Uhlenbeck and S. Goudsmit, *Nature* **117** (1926) 248.
2. A. Pais, *George Uhlenbeck and the discovery of electron spin*, na, (1989).
3. G. E. Uhlenbeck and S. Goudsmit, Spinning Electrons and the Structure of Spectra *Nature* **117** (1926) 264. https://doi.org/10.1038/117264a0
4. J. Barnaś and A. Fert, *Phys. Rev. Lett.* **80** (1998) 1058. https://doi.org/10.1103/PhysRevLett.80.1058
5. H. Munekata, H. Ohno, S. Von Molnar, A. Segmüller, L. L. Chang and L. Esaki, *Phys. Rev. Lett.* **63** (1989) 1849. https://doi.org/10.1103/PhysRevLett.63.1849
6. M. Berber, B. Doumi, A. Mokaddem, Y. Mogulkoc, A. Sayede and A. Tadjer, *J. Electron. Mater.* **47** (2018) 449. https://doi.org/10.1007/s11664-017-5793-1
7. A. Laroussi *et al.*, First-Principles Calculations of the Structural, Electronic and Magnetic Properties of Mn-Doped InSb by Using mBJ Approximation for Spintronic Application, Acta *Acta Phys. Pol. A.* **135** (2019) 451. doi:10.12693/APhysPolA.135.451

8. B. Beber *et al*., Improved Electronic Structure and Optical Performance of Bi2Te3-xSex From First-principle Calculations Within TB-mBJ Exchange Potential, *Mater. Res.* **21** (2018). http://dx.doi.org/10.1590/1980-5373-mr-2017-0553.
9. M. Berber et al., Investigation of electronic structure and half-metallic ferromagnetic behavior with large half-metallic gap in Sr1-xVxO, *J. Comput. Electron.* **16** (2017) 542. https://doi.org/10.1007/s10825-017-1038-z.
10. A. Laroussi *et al*., The effect of substitution of Cr impurities at the In sites on the structural, electronic and magnetic properties of InSb: a DFT study within mBJ potential, *Appl. Phys. A* **125** (2019) 676. https://doi.org/10.1007/s00339-019-2973-2.
11. S. Berri, A. Kouriche, D. Maouche, F. Zerarga and M. Attallah, Ab initio study of electronic structure and magnetic properties in ferromagnetic Sr1-x(Mn, Cr)xO alloys, *Mater. Sci. Semicond. Process.* **38** (2015) 101. https://doi.org/10.1016/j.mssp.2015.04.016
12. B. Doumi *et al*., First-principle investigation of half-metallic ferromagnetism in octahedrally bonded Cr-doped rock-salt SrS, SrSe, and SrTe, *Eur. Phys. J. B* **88**, doi:10.1140/epjb/e2015-50746-9.
13. M. I. Khan *et al*., Investigation of structural, electronic, magnetic and mechanical properties of a new series of equiatomic quaternary Heusler alloys CoYCrZ (Z = Si, Ge, Ga, Al): A DFT study, *J. Alloys Compd*. **819** (2020) 152964. https://doi.org/10.1016/j.jallcom.2019.152964.
14. A. Aryal *et al*., Effect of Bi substitution on the magnetic and magnetocaloric properties of Ni50Mn35In15-xBix Heusler alloys, AIP Advances. MMM2018 (2018) 056409, https://doi.org/10.1063/1.5004694@adv.2018.MMM2018.issue-1
15. T. Kanomata *et al*., Magnetic properties of ferromagnetic Heusler alloy Co2NbGa, *J. Magn. Magn. Mater*. **503** (2020) 166604. https://doi.org/10.1016/j.jmmm.2020.166604.
16. T. Roy, M. Tsujikawa, T. Kanemura and M. Shirai, *J. Magn. Magn. Mater.* **498** (2020) 166092. https://doi.org/10.1016/j.jmmm.2019.166092.
17. G. Forozani, A. A. M. Abadi, S. M. Baizaee and A. Gharaati, Structural, electronic and magnetic properties of CoZrIrSi quaternary Heusler alloy: First-principles study, *J. Alloys Compd*. **815** (2020) 152449. https://doi.org/10.1016/j.jallcom.2019.152449
18. D. Král *et al*., Magnetic and Magneto-Optical Properties of Fe75-xMn25Gax Heusler-like Compounds, *Materials (Basel)*. **13** (2020) 703. https://doi.org/10.3390/ma13030703
19. J. Mašek Mn-doped Ga(As,P) and (Al,Ga)As ferromagnetic semiconductors: Electronic structure calculations *Phys. Rev. B* **75** (2007) 45202. https://doi.org/10.1103/PhysRevB.75.045202
20. F. Bantien and J. Weber, Properties of the optical transitions within the Mn acceptor in AlxGa1-xAs, *Phys. Rev. B* **37** (1988) 10111. https://doi.org/10.1103/PhysRevB.37.10111
21. K. Schwarz, DFT calculations of solids with LAPW and WIEN2k, *J. Solid State Chem*. **176** (2003) 319. https://doi.org/10.1016/S0022-4596(03)00213-5
22. P. Blaha, K. Schwarz, G. K. H. Madsen, D. Kvasnicka and J. Luitz, *An Augment. Pl. wave+ local orbitals Progr. Calc. Cryst. Prop*.
23. K. Schwarz, P. Blaha and G. K. H. Madsen, Electronic structure calculations of solids using the WIEN2k package for material sciences, *Comput. Phys. Commun*. **147** (2002) 71. https://doi.org/10.1016/S0010-4655(02)00206-0.
24. G. K. H. Madsen, P. Blaha, K. Schwarz, E. Sjöstedt and L. Nordström, Efficient linearization of the augmented plane-wave method, *Phys. Rev. B* **64** (2001) 195134. https://doi.org/10.1103/PhysRevB.64.195134
25. J. P. Perdew, K. Burke and M. Ernzerhof, Generalized Gradient Approximation Made Simple, *Phys. Rev. Lett.* **77** (1996) 3865. https://doi.org/10.1103/PhysRevLett.77.3865
26. F. Tran and P. Blaha, Accurate Band Gaps of Semiconductors and Insulators with a Semilocal Exchange-Correlation Potential, *Phys. Rev. Lett*. **102** (2009) 226401. https://doi.org/10.1103/PhysRevLett.102.226401
27. E. I. Rashba, Theory of electrical spin injection: Tunnel contacts as a solution of the conductivity mismatch problem, *Sov. Physics, Solid State* **2** (1960) 1109. https://doi.org/10.1103/PhysRevB.62.R16267
28. H. Lefebvre-Brion and R. W. Field, *The Spectra and Dynamics of Diatomic Molecules*: Revised and Enlarged Edition, (Elsevier, 2004).
29. P. F. Bernath, *Spectra of atoms and molecules*, (Oxford university press, 2020).
30. A. Bautista-Hernandez, T. Rangel, A. H. Romero, G.-M. Rignanese, M. Salazar-Villanueva and E. Chigo-Anota, Structural and vibrational stability of M and Z phases of silicon and germanium from first principles, *J. Appl. Phys*. **113** (2013) 193504. https://doi.org/10.1063/1.4804668
31. Michael J. Mehl, Pressure dependence of the elastic moduli in aluminum-rich Al-Li compounds, *Phys. Rev. B* **47** (1993) 2493. https://doi.org/10.1103/PhysRevB.47.2493
32. G. V Sin'Ko and N. A. Smirnov, Ab initio calculations of elastic constants and thermodynamic properties of bcc, fcc, and hcp Al crystals under pressure, *J. Phys. Condens. Matter* **14** (2002) 6989. https://doi.org/10.1088/0953-8984/14/29/301
33. P. Wachter, M. Filzmoser and J. Rebizant, Electronic and elastic properties of the light actinide tellurides, *Phys. B Condens. Matter* **293** (2001) 199. https://doi.org/10.1016/S0921-4526(00)00575-5
34. O. L. Anderson, A simplified method for calculating the debye temperature from elastic constants, *J. Phys. Chem. Solids* **24** (1963) 909. https://doi.org/10.1016/0022-3697(63)90067-2
35. E. Schreiber, O. L. Anderson and N. Soga, *Elastic constants and their measurement*, McGraw-Hill New York, (1973), **vol. 6**.
36. S. F. Pugh, London, Edinburgh, Relations between the elastic moduli and the plastic properties of polycrystalline pure metals. *Dublin Philos. Mag. J. Sci*. **45** (1954) 823. https://doi.org/10.1080/14786440808520496